Anisotropic density fluctuations in argon at different densities: Far infrared measurements and molecular dynamic calculations

D. Frenkel[a] and J. van der Elsken

Laboratory for Physical Chemistry, University of Amsterdam, Nieuwe Prinsengracht 126, Amsterdam, The Netherlands
(Received 21 June 1977)

From measurements of the pure rotational lines of a linear probe molecule dissolved in a simple fluid one can deduce the power spectra of the anisotropic density fluctuations of $l = 1$ and $l = 2$ symmetry of the fluid. The power spectra thus obtained for argon at various densities are compared with the results of molecular dynamics calculations and with the approximate power spectra which can be calculated starting from neutron-scattering data. The density dependence of the high frequency components of the $l = 1$ power spectrum and of the zero frequency component of the $l = 2$ power spectrum give a strong characteristic of the dense fluid.

INTRODUCTION

The rotational relaxation of a linear, quantized rotor molecule imbedded in a fluid is completely determined by the anisotropic density fluctuations of that fluid. Information about such fluctuations can therefore be obtained from a study of the relaxation. Any technique which probes a molecular relaxation process provides us with macroscopic measurements, and the information which can be obtained is therefore a statistically averaged property. Inelastic neutron scattering for instance yields information on the dynamic pair–correlation function. The rotational relaxation of a probe molecule in a single fluid gives likewise information about this type of density correlation functions.

If one wants to compare different pieces of information about density correlations in a fluid, it is favorable to choose argon as an example. Coherent and incoherent neutron scattering data are available for argon at different densities, molecular dynamics calculations on the time dependence of anisotropic potentials have been performed, and the authors recently published the results of an experimental study of the rotational relaxation of the dipole molecule HCl as probe molecule in argon of different densities, along the 162 K isotherm. In the gradual transition from gas densities (around the critical point) to densities typical for the liquids, the anisotropic density fluctuations of the system must undergo a very drastic change. The investigation of this process is the purpose of the work reported here. We will first of all show how the local anisotropy and rotational relaxation are connected and in particular how line broadening can be used to find the correlation functions of the anisotropic perturbations acting on the probe molecule. Subsequently, we will show how a comparison can be made with neutron scattering data. In combination with results from molecular dynamics (MD) calculations on a Lennard-Jones system simulating argon we can draw some conclusions about the change of the microdynamic processes with increasing density in the argon fluid.

[a]Present address: Department of Chemistry, University of California, Los Angeles, California.

I. DENSITY FLUCTUATIONS AND LINE BROADENING

The interaction energy between a linear molecule and a perturbing atom may quite generally be written as

$$V(1_\mu) = \sum_{l=0}^{\infty} v_l(r)\, P_l(1_r \cdot 1_\mu), \tag{1}$$

where $v_l(r)$ gives the r-dependence of that part of the molecule–perturber potential that transforms as the lth Legendre polynomial. 1_r is the unit vector in the direction of the line joining the centers of mass of the molecule and the perturber, and 1_μ is the unit vector along the molecular axis. Making the crucial assumption that the time dependence of all translational coordinates is independent of the rotational coordinate of the probe, the time dependence of $V(1_\mu)$ may be obtained, once the equations of motion that govern the translational coordinates have been solved. Computing the time dependence of $V(1_\mu)$ is of course greatly facilitated if the translational motions may be treated classically. By inserting the now explicitly time-dependent perturbation in the Schrödinger equation of the rotor, one may calculate the time-evolution operator for the dipole molecule, and hence, for an isolated collision, the S matrix. The S matrix completely determines the effect of a given collision on the rotational motion of the molecule. We will not restrict ourselves to the case of a molecule perturbed by a single atom, but rather look directly at the more general case in which the molecule feels the influence of more than one perturber at a time. At this point we will make the assumption that the intermolecular potential is pairwise additive. Under this restriction, the total perturbation may be written as

$$V(1_\mu) = \sum_{i=1}^{N} \sum_{l=0}^{\infty} v_l(r_i) \frac{4\pi}{2l+1} \sum_{m=-l}^{l} Y^*_{lm}(1_{r_i})\, Y_{lm}(1_\mu), \tag{2}$$

where $\mathbf{r}_i$ denotes the coordinates of perturber i, with respect to the center of mass of the perturbed molecule. Writing the number density at distance $\mathbf{r}$ from the probe as $\rho(\mathbf{r}) = \sum_{i=1}^{N} \delta(\mathbf{r} - \mathbf{r}_i)$, the above equation may be written as

$$V(1_\mu) = \sum_{l=0}^{\infty} \frac{4\pi}{2l+1} \sum_{m=-l}^{l} Y_{lm}(1_\mu) \int d\mathbf{r}\, \rho(\mathbf{r})\, v_l(r)\, Y^*_{lm}(1_r). \tag{3}$$

As we assumed the translational motions to be independent of the state of the rotor, $\rho(\mathbf{r})$ is explicitly time dependent, and the perturbation acting on the probe molecule has the following form

$$V(1_\mu;\, t) = \sum_{l=0}^{\infty} \frac{4\pi}{2l+1} \sum_{m=-l}^{l} a_{lm}(t)\, Y_{lm}(1_\mu), \tag{4}$$

with

$$a_{lm}(t) \equiv \int d\mathbf{r}\, \rho(\mathbf{r})\, v_l(r)\, Y^*_{lm}(1_r).$$

The strength and the time dependence of the perturbation are determined by the local density fluctuations around the probe; in particular, the symmetry and range of the intermolecular potential determines the symmetry and range of the density fluctuations that couple to the rotational motion.[1]

The dipole correlation function is defined by

$$\langle \mu(0) \cdot \mu(t) \rangle = \mathrm{Tr}\left[\rho \mu U^+(t)\, \mu U(t)\right]. \tag{5}$$

$U(t)$ is the time evolution operator which determines the state vector at time t in terms of the state vector at time 0. Written in the interaction picture it is explicitly given by

$$U(t, t_0) = e^{iH_0 t/\hbar} e^{-iH(t-t_0)/\hbar} e^{-iH_0 t_0/\hbar},$$

where the total Hamiltonian $H(t) = H_0 + V(t)$. The equation of motion is

$$\frac{\partial}{\partial t} U(t) = \frac{-i}{\hbar} V(t)\, U(t). \tag{6}$$

A solution may be obtained by iterated integration once the explicit time dependence of $\rho(\mathbf{r})$ is known. Once this solution is found, the dipole moment correlation function can be calculated by inserting $\mu(t) = U^+(t)\, \mu U(t)$ and performing the averaging over the translational coordinates.

There is, however, a problem connected with the fact that the perturbation acting on the probe is explicitly time dependent. Such a perturbation does not maintain thermal equilibrium, but rather tends to heat up the rotational degrees of freedom. We will neglect the effect of this heating up on the density matrix of the molecule in assuming that, even if the perturbation is acting on the molecule, the density matrix is still equal to the density matrix of the free rotor. For cases in which the perturbation contains a very large, almost static part, Robert and Galatry[2] suggested a different approach in which the density matrix is diagonalized in a new basis. More recent work by Hoang[3] does, however, seem to indicate that in the case of HCl dissolved in noble gas solvents the nondiagonality of the density matrix is of little importance. Using this assumption, the dipole correlation function may be written in the following way

$$\begin{aligned}
\langle \mu(0) \cdot \mu(t) \rangle &= \rho_i \left[\langle i \,|\, \mu U^\dagger(t)\, \mu U(t) \,|\, i \rangle \right]_{\mathrm{av}} \\
&= \rho_i \Big[\langle i|\mu|j\rangle \langle j \,|\, 1 + i/\hbar \int_0^t V_I(t')\, dt' - 1/\hbar^2 \int_0^t \int_0^{t'} V_I(t'')\, V_I(t')\, dt'\, dt'' + \cdots \,|\, k \rangle \\
&\quad \cdot \langle k \,|\, e^{iH_0 t/\hbar} \mu\, e^{-iH_0 t/\hbar} \,|\, l \rangle \langle l \,|\, 1 - i/\hbar \int_0^t V_I(t')\, dt' - 1/\hbar^2 \int_0^t \int_0^{t'} V_I(t')\, V_I(t'')\, dt'\, dt'' + \cdots \,|\, i \rangle \Big]_{\mathrm{av}},
\end{aligned} \tag{7}$$

We will only retain those elements of the time-evolution operator that are diagonal in the energy ($E_j = E_k$ and $E_i = E_l$). For a linear rotor this implies that we neglect all elements of $U(t)$ that connect states of different j. In general, off-diagonal elements of the time-evolution operator may give nonnegligible contributions to the dipolar absorption spectrum. Neilsen and Gordon[4] have concluded from an impact calculation on rotational line broadening of HCl by argon, that off-diagonal elements of the σ matrix have little influence on the spectral shape for Ar densities below 1500 amagat. As the off-diagonal elements of the σ matrix contain the off-diagonal terms of the time-evolution operator, this implies that, within the impact approximation, off-diagonal elements of $U(t)$ may be neglected for all densities that are experimentally accessible. It should be expected that this will not only hold for the HCl argon system, but in general for systems that exhibit features characteristic for quantized rotations and hence for the systems under consideration. Although we do not work within the impact approximation, and therefore may expect to get a somewhat different estimate of the relative importance of off-diatonal elements of $U(t)$, there is little reason to expect dramatically different results. We obtain

$$\begin{aligned}
\langle \mu(0) \cdot \mu(t) \rangle &= (2j+1)^{-1} \rho_j \exp(i\omega_{jt}\, t) \cdot \Big[\langle jm \,|\, \mu \,|\, j'm' \rangle \langle j'm' \,|\, 1 + i/\hbar \int_0^t V_I(t')\, dt' \\
&\quad - 1/\hbar^2 \int_0^t \int_0^{t'} V_I(t'')\, V_I(t')\, dt'\, dt'' + \cdots \,|\, j'm'' \rangle \langle j'm'' \,|\, \mu \,|\, jm''' \rangle \\
&\quad \times \langle jm''' \,|\, 1 - i/\hbar \int_0^t V_I(t')\, dt' - 1/\hbar^2 \int_0^t \int_0^{t'} V_I(t')\, V_I(t'')\, dt'\, dt'' + \cdots \,|\, jm \rangle \Big]_{\mathrm{av}},
\end{aligned} \tag{8}$$

where

$$\rho_j = \sum_{m=-j}^{j} \exp(-\beta E_j) \Big/ \sum_{j',m'} \exp(-\beta E_{j'}).$$

Making use of the Wigner–Eckart theorem,[5] the m dependence of the matrix elements of μ may be worked out

$$\langle \mu(0)\cdot\mu(t)\rangle = (2j+1)^{-1}\rho_j(-1)^q(-1)^{j-m}$$
$$\cdot\begin{pmatrix} j & 1 & j' \\ -m & q & m'\end{pmatrix}\langle j\|\mu\|j'\rangle(-1)^{j'-m'}\begin{pmatrix} j' & 1 & j \\ -m'' & -q & m'''\end{pmatrix}$$
$$\cdot\langle j'\|\mu\|j\rangle\exp(i\omega_{j'j}t)[\langle j'm'\,|\,U_I^\dagger(t)\,|\,j'm''\rangle\langle jm'''|\,U_I(t)\,|jm\rangle]_{\rm av}. \tag{9}$$

The average $\langle j'm'\mid U_I^\dagger(t)\mid j'm''\rangle\langle jm'''\mid U_I(t)\mid jm\rangle$ may be expanded

$$\Big\{\delta_{m',m''}\delta_{m''',m}+i/\hbar\,\delta_{m''',m}\int_0^t[\langle j'm'\,|\,V_I(t')\,|j'm''\rangle]_{\rm av}dt'+-i/\hbar\,\delta_{m',m''}\int_0^t[\langle jm'''|\,V_I(t')\,|jm\rangle]_{\rm av}dt'$$
$$+1/\hbar^2\int_0^t\int_0^{t'}[\langle j'm'\,|\,V_I(t')|j'm''\rangle\langle jm'''\,|\,V_I(t'')\,|jm\rangle]_{\rm av}dt'\,dt''$$
$$-1/\hbar^2\,\delta_{m',m''}\int_0^t\int_0^{t'}[\langle jm'''\,|\,V_I(t')\,V_I(t'')\,|jm\rangle]_{\rm av}dt'\,dt''-1/\hbar^2\,\delta_{m''',m}\int_0^t\int_0^{t'}$$
$$\times[\langle j'm'\,|\,V_I(t'')\,V_I(t')\,|\,j'm''\rangle]_{\rm av}dt'\,dt''+\cdots\Big\}. \tag{10}$$

As the fluid around the probe is on the average isotropic, all terms in the above expression that are linear in $V(t)$ vanish. Up to second order in V, we are therefore left with terms that involve correlation functions of the perturbing potential. To be more precise, as $V(t)=\sum_{l,m}(4\pi/2l+1)\,a_{lm}(t)\,Y_{lm}(\mathbf{1}_\mu)$, the relevant correlation functions are the correlation functions of $a_{lm}(t)$. Due to the isotropy of the fluid, all $\langle a_{lm}(0)\,a_{l'm'}(t)\rangle$ vanish, unless $l=l'$ and $m=m'$, whereas

$$\langle a_{lm}(0)\,a_{l-m}(t)\rangle = \int\int d\mathbf{r}\,d\mathbf{r}'\,\langle\rho(\mathbf{r};0)\rho(\mathbf{r}';t)\rangle\,v_l(r)\,v_l(r')\,Y^*_{lm}(\mathbf{1}_r)\,Y^*_{l-m}(\mathbf{1}_{r'})$$
$$=(-1)^m\int\int d\mathbf{r}\,d\mathbf{r}'\,\langle\rho(\mathbf{r};0)\rho(\mathbf{r}';t)\rangle\,v_l(r)\,v_l(r')\,Y^*_{lm}(\mathbf{1}_r)\,Y_{lm}(\mathbf{1}_{r'})$$
$$=(-1)^m(2l+1)^{-1}\sum_{m'=-l}^{l}\int\int d\mathbf{r}\,d\mathbf{r}'\langle\rho(\mathbf{r};0)\rho(\mathbf{r}';t)\rangle\,v_l(r)\,v_l(r')\,Y^*_{lm'}(\mathbf{1}_r)\,Y_{lm'}(\mathbf{1}_{r'})$$
$$=(-1)^m(4\pi)^{-1}\int\int dr\,dr'\,\langle\rho(\mathbf{r};0)\rho(\mathbf{r}';t)\rangle\,v_l(r)\,v_l(r')\,P_l(\mathbf{1}_r\cdot\mathbf{1}_{r'}). \tag{11}$$

Apart from a factor $(-1)^m$, $\langle a_{lm}(0)\,a_{l-m}(t)\rangle$ is determined by an integral which is independent of m. We now define a function $g_l(t)$ by

$$g_l(t)\equiv\int\int d\mathbf{r}\,d\mathbf{r}'\langle\rho(\mathbf{r};0)\rho(\mathbf{r}';t)\rangle\,v_l(r)\,v_l(r')\,P_l(\mathbf{1}_r\cdot\mathbf{1}_{r'}) \tag{12}$$

The entire m dependence in Eq. (9) may now be removed making use of the properties of $3J$ and $6J$ symbols.[5]

$$\langle\mu(0)\cdot\mu(t)\rangle=\rho_j\langle j\|\mu\|j'\rangle^2\exp(i\omega_{j'j}t)\Big[1-1/\hbar^2\sum_{l=0}^{\infty}(2l+1)\Big]^{-1}$$
$$\cdot\Big\{\int_0^t\int_0^{t'}g_l(t''-t')\Big[(2j+1)\begin{pmatrix} j & l & j\\ 0&0&0\end{pmatrix}^2+(2j'+1)\begin{pmatrix} j' & l & j'\\ 0&0&0\end{pmatrix}^2-2(-1)^{x-l}(2j+1)(2j'+1)$$
$$\cdot\begin{pmatrix} j' & l & j'\\ 0&0&0\end{pmatrix}\begin{pmatrix} j & l & j\\ 0&0&0\end{pmatrix}\begin{pmatrix} j' & j & x\\ j & j' & l\end{pmatrix}\Big]dt'\,dt''$$
$$+\int_0^t\int_0^{t'}g_l(t''-t')\sum_{j_f\neq j}(2j_f+1)\begin{pmatrix} j & l & j_f\\ 0&0&0\end{pmatrix}^2\exp[i\omega_{j_fj}(t''-t')]\,dt'\,dt''$$
$$+\int_0^t\int_0^{t'}g_l(t''-t')\sum_{j_f\neq j'}(2j_f+1)\begin{pmatrix} j' & l & j'\\ 0&0&0\end{pmatrix}^2\exp[i\omega_{j'j_f}(t''-t')]\,dt'\,dt''\Big\}+\cdots. \tag{13}$$

In fact, Eq. (13) is the expression for the correlation function of an arbitrary molecular property that transforms as an irreducible tensor of rank X. The dipole correlation function is obtained for $X=1$. We now assume that the expression above represents the first few terms of a series expansion of a correlation function of the following form

$$\langle\mu(0)\cdot\mu(t)\rangle=\rho_j\langle j\|\mu\|j'\rangle^2\exp(i\omega_{j'j}t)\exp\Big[-1/\hbar^2\sum_{l=0}^{\infty}(2l+1)\Big]^{-1}\Big\{\int_0^t\int_0^{t'}g_l(t''-t')\Big[(2j+1)\begin{pmatrix} j & l & j\\ 0&0&0\end{pmatrix}^2+(2j'+1)$$
$$\cdot\begin{pmatrix} j' & l & j'\\ 0&0&0\end{pmatrix}^2-2(-1)^{x-l}(2j+1)(2j'+1)\begin{pmatrix} j' & l & j'\\ 0&0&0\end{pmatrix}\begin{pmatrix} j & l & j\\ 0&0&0\end{pmatrix}\begin{pmatrix} j' & j & x\\ j & j' & l\end{pmatrix}\Big]dt'\,dt''$$

$$+\int_0^t \int_0^{t'} g_l(t''-t') \sum_{j_f \neq j} (2j_f+1)\begin{pmatrix} j & l & j_f \\ 0 & 0 & 0 \end{pmatrix}^2 \exp[i\omega_{j_f j}(t''-t')]\, dt'\, dt''$$
$$+\int_0^t \int_0^{t'} g_l(t''-t') \sum_{j_f \neq j'} (2j_f+1)\begin{pmatrix} j' & l & j_f \\ 0 & 0 & 0 \end{pmatrix}^2 \exp[i\omega_{j' j_f}(t''-t')] \Bigg\}. \tag{14}$$

In shorthand notation

$$\langle \mu(0)\cdot\mu(t)\rangle = \rho_j \langle j \| \mu \| j' \rangle^2 \exp(i\omega_{j'j}t)\exp[-\gamma_{j'j}(t)]. \tag{14a}$$

The last line defines the damping function $\gamma_{j'j}(t)$. This expression for the correlation function may be obtained in a straightforward way as the lowest order approximation to the cumulant expansion of Eq. (9).[6] It is valid as long as higher-order cumulants may be neglected or, equivalently, as long as the perturbation is a Gaussian process. The validity of this assumption is hard to assess. To investigate the statistical properties of the perturbing potential in more detail, a molecular dynamics experiment seems best suited. Although the authors have published molecular dynamics calculations on the perturbing potential,[7] they did not test whether the perturbation behaved as a Gaussian process. The question therefore remains open.

Limiting time behavior

For times long compared with the decay time of all $g_l(t)$, $\gamma_{j'j}(t)$ may be approximated by

$$\gamma_{j'j}(t) \simeq \hbar^{-2} t \sum_{l=0}^{\infty} (2l+1)^{-1} \Bigg\{ \int_0^{\infty} g_l(\tau) \Bigg[(2j+1)\begin{pmatrix} j & l & j \\ 0 & 0 & 0 \end{pmatrix}^2 + (2j'+1)\begin{pmatrix} j' & l & j' \\ 0 & 0 & 0 \end{pmatrix}^2$$
$$+ -2(-1)^{x-l}(2j+1)(2j'+1)\begin{pmatrix} j' & l & j' \\ 0 & 0 & 0 \end{pmatrix}\begin{pmatrix} j & l & j \\ 0 & 0 & 0 \end{pmatrix}\begin{pmatrix} j & j & x \\ j' & j' & l \end{pmatrix}\Bigg] d\tau$$
$$+ \int_0^{\infty} g_l(\tau) \sum_{j_f \neq j} (2j_f+1)\begin{pmatrix} j & l & j_f \\ 0 & 0 & 0 \end{pmatrix}^2 \exp(i\omega_{j_f j}\tau)\, d\tau + \int_0^{\infty} g_l(\tau) \sum_{j_f j'} (2j_f+1)\begin{pmatrix} j' & l & j_f \\ 0 & 0 & 0 \end{pmatrix}^2 \exp(i\omega_{j' j_f}\tau)\, d\tau \Bigg\} \equiv \Gamma_{j'j} t. \tag{15}$$

Consequently, the dipole correlation function reduces to a sum of exponentials as $t \to \infty$

$$\langle \mu(0)\cdot\mu(t)\rangle = \rho_j \langle j \| \mu \| j' \rangle^2 \exp[(i\omega_{j'j} - \Gamma_{j'j})t]. \tag{16}$$

If the decay time of all $g_l(t)$ is much smaller than $\Gamma_{j'j}^{-1}$, Eq. (16) is a good approximation for the dipole correlation function for all t. In general, this condition will be met in the limit of weak anisotropic perturbations, because $\Gamma \to 0$ as the size of anisotropic potential fluctuations goes to zero. In that case, the dipole moment power spectrum consists of a sum of Lorentzians with width $\mathrm{Re}\Gamma_{j'j}$ and shift $\mathrm{Im}\Gamma_{j'j}$. The $\Gamma_{j'j}$ may be expressed in terms of the Laplace transforms of the $g_l(t)$

$$\Gamma_{j'j} = \hbar^2 \sum_{l=0}^{\infty} (2l+1)^{-1} \Bigg\{ G_l(0) \Bigg[(2j+1)\begin{pmatrix} j & l & j \\ 0 & 0 & 0 \end{pmatrix}^2 + (2j'+1)$$
$$\cdot \begin{pmatrix} j' & l & j' \\ 0 & 0 & 0 \end{pmatrix}^2 + -2(-1)^{x-l}(2j+1)(2j'+1)$$
$$\times \begin{pmatrix} j' & l & j' \\ 0 & 0 & 0 \end{pmatrix}\begin{pmatrix} j & l & j \\ 0 & 0 & 0 \end{pmatrix}\begin{pmatrix} j' & j & x \\ j & j' & l \end{pmatrix}\Bigg]$$
$$+ \sum_{j_f \neq j} G_l(\omega_{j j_f})(2j_f+1)\begin{pmatrix} j & l & j_f \\ 0 & 0 & 0 \end{pmatrix}^2$$
$$+ \sum_{j_f \neq j'} G_l(\omega_{j_f j'})(2j_f+1)\begin{pmatrix} j' & l & j_f \\ 0 & 0 & 0 \end{pmatrix}^2 \Bigg\}$$

with

$$G_l(\omega) = \int_0^{\infty} \exp(-i\omega t) g_l(t)\, dt. \tag{17}$$

The width and shift of the different rotational lines are therefore linear combinations of the Laplace transforms of the correlation functions of the anisotropic perturbations acting on the probe molecule. In fact, it is a linear combination of the values of all $G_l(\omega)$ at frequencies that correspond to the level spacings in the unperturbed rotor.

Although the sum in Eq. (17) runs over all l from 0 to ∞, the isotropic perturbation ($l=0$), of course, does not contribute to rotational relaxation, the concerning contributions do indeed vanish.

It should be noticed that the line broadening may be written as the sum of a term that contains the $\omega = 0$ components of the perturbation, i.e.,

$$\mathrm{Re}\,\Gamma_{j'j}(\omega=0) = \hbar^{-2} \sum_{l=0}^{\infty} (2l+1)^{-1} G_l(0) \Bigg[(2j+1)\begin{pmatrix} j & l & j \\ 0 & 0 & 0 \end{pmatrix}^2$$
$$+ (2j'+1)\begin{pmatrix} j' & l & j' \\ 0 & 0 & 0 \end{pmatrix}^2 + -2(-1)^{x-l}(2j+1)$$
$$\times (2j'+1)\begin{pmatrix} j' & l & j' \\ 0 & 0 & 0 \end{pmatrix}\begin{pmatrix} j & l & j \\ 0 & 0 & 0 \end{pmatrix}\begin{pmatrix} j' & j & x \\ j & j' & l \end{pmatrix}\Bigg], \tag{18}$$

plus a term that contains only nonzero frequency components

$$\mathrm{Re}\,\Gamma_{j'j}(\omega \neq 0) = \hbar^{-2}\,\mathrm{Re} \sum_{l=0}^{\infty} (2l+1)^{-1} \Bigg[\sum_{j_f \neq j} G_l(\omega_{j j_f})(2j_f+1)$$
$$\times \begin{pmatrix} j & l & j_f \\ 0 & 0 & 0 \end{pmatrix}^2 + \sum_{j_f \neq j'} G_l(\omega_{j_f j'})(2j_f+1)\begin{pmatrix} j' & l & j_f \\ 0 & 0 & 0 \end{pmatrix}^2 \Bigg]. \tag{19}$$

The shift is exclusively determined by finite-frequency components

$$\mathrm{Im}\,\Gamma_{j',j} = \hbar^{-2}\,\mathrm{Im}\sum_{l=0}^{\infty}(2l+1)^{-1}\cdot\Big[\sum_{j_f\neq j} G_l(\omega_{jj_f})(2j_f+1)\times\begin{pmatrix} j & l & j_f\\ 0 & 0 & 0\end{pmatrix}^2 + \sum_{j_f\neq j'} G_l(\omega_{j_fj'})(2j_f+1)\begin{pmatrix} j' & l & j_f\\ 0 & 0 & 0\end{pmatrix}^2\Big]. \tag{20}$$

If the rotational spacing of a molecule is large with respect to the characteristic frequencies of the perturbing potential (H_2 in argon seems to be a likely candidate), the line broadening is determined almost exclusively by the $G_l(0)$ and the shift may be expected to be quite small. If, on the other hand, the rotational spacings of the probe molecule cover the entire frequency range of the fluctuating anisotropic potential, the finite-frequency components of the perturbation will certainly contribute to the rotational relaxation. Such may be expected to be the case in the HCl-Ar system, a system of which we use the results in Sec. II.

II. FOUR POINT DENSITY CORRELATION FUNCTIONS

Density fluctuations and the power spectra of anisotropic perturbations are contained in the density–density correlation functions $\langle\rho(\vec{r};0)\rho(\vec{r}';t)\rangle$. This correlation function relates the density at distance $\vec{r}$ from a labeled particle at $t=0$ to the density at $\vec{r}'$ at time t. Actually

$$\langle\rho(\mathbf{r};0)\rho(\mathbf{r}';t)\rangle = \int\int d\mathbf{R}\,d\mathbf{R}' \times\langle n_L(\mathbf{R};0)n_u(\mathbf{R}+\mathbf{r};0)n_L(\mathbf{R}';t)n_u(\mathbf{R}'+\mathbf{r}';t)\rangle\,, \tag{21}$$

where n_L and n_u denote the number densities of certain labeled particles and of the other particles.

$n_L(\mathbf{R}) = \delta(\mathbf{R}-\mathbf{R}_L)$ and $n_u(\mathbf{R}) = \sum_{i=1}^{N}\delta(\mathbf{R}-\mathbf{R}_u^i)$. Since $\mathbf{r}$ and $\mathbf{r}'$ are relative distances, the correlation function depends on four independent variables.

It is useful to define

$$(4\pi)^{-1}\int d\Omega\,\langle\rho(\mathbf{r};0)\rho(\mathbf{r}';t)\rangle P_l(1_r\cdot 1_{r'}) \equiv \langle\rho(\mathbf{r};0)(\mathbf{r};t)\rangle_l\,, \tag{22}$$

where the angular part has been integrated out so that only three variables remain. It is this latter correlation function (mainly with $l=1$ and $l=2$) which determines the power spectra of anisotropic perturbations playing a role in the rotational relaxation of a linear molecule in a noble gas and in collision induced dipolar absorption such as found in noble gas mixtures. In the first case, the linear molecule is assumed to play the part of the labeled particle. In Sec. I we have shown that there is a linear relation between the width and the shift of rotational absorption lines and the correlation functions. In the latter case (CIDA) the spectral intensity is determined by the correlation function of the collision induced dipole

$$\mu_{\mathrm{ind}}(0)\,\mu_{\mathrm{ind}}(t)\rangle = \int\int d\mathbf{r}\,d\mathbf{r}'\langle\rho(\mathbf{r};0)\rho(\mathbf{r}';t)\rangle \times\mu(\mathbf{r})\mu(\mathbf{r}')P_1(1_r\cdot 1_{r'})\,, \tag{23}$$

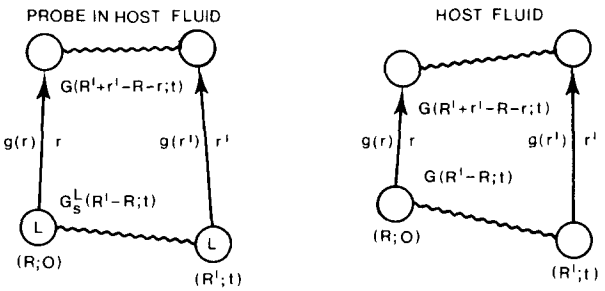

FIG. 1. Approximations for the four-point density correlation function according to Eqs. (26) and (27). Straight lines indicate distances at equal times, wiggly lines apply to distances in space and time.

where $\rho(\mathbf{r};0)$ denotes the density of the host fluid at distance $\mathbf{r}$ from the dissolved noble gas atom. Since $g'(t) = \int\int d\mathbf{r}\,d\mathbf{r}'\langle\rho(\mathbf{r};0)\rho(\mathbf{r}';t)\rangle v_1(r)v_1(r')P_1(1_r\cdot 1_{r'})$ the only difference between $\langle\mu_{\mathrm{ind}}(0)\,\mu_{\mathrm{ind}}(t)\rangle$ and $g_1(t)$ is that the former is given by an integral over the correlation function weighted by $\mu(r)\,\mu(r')$, whereas in the latter the same correlation function is multiplied by $v_1(r)\,v_1(r')$. The collision induced dipoles have a very short range. Density fluctuations of P_1 symmetry sensed by a CIDA experiment are therefore of a much shorter range around the probe atom than the P_1 fluctuations found from line-broadening measurements with a probe molecule. Both measurements may nicely complement one another.

A slightly different four point density correlation function plays a role in collision induced depolarized light scattering (CILS). Such scattering may be measured in pure noble gas fluid, the intensity is given by

$$I \sim \int\int d\mathbf{r}\,d\mathbf{r}'\langle\rho'(\mathbf{r};0)\rho'(\mathbf{r}';t)\rangle\,\beta(r)\beta(r')\,P_2(1_r\cdot 1_{r'}) \tag{24}$$

where $\beta(r)$ is the magnitude of the collision induced polarizability tensor which for large r depends on r like r^{-3}. The CILS measurements probe the density fluctuations of P_2 symmetry given by the correlation function

$$\langle\rho'(\mathbf{r};0)\rho'(\mathbf{r}';t)\rangle \equiv N^{-2}\int\int d\mathbf{R}\,d\mathbf{R}' \times\langle n(\mathbf{R};0)n(\mathbf{R}+\mathbf{r};0)n(\mathbf{R}';t)n(\mathbf{R}'+\mathbf{r}';t)\rangle\,, \tag{25}$$

where no labeling occurs.

There also exists the possibility to connect the four point density correlation functions of the type used here with the lower order density correlation functions such as may be measured with neutron scattering experiments. Approximate models have been proposed for both types.[8–10] We will use an approximation which resembles the Vineyard approximation,[11] illustrated by Fig. 1.

$$\langle n_L(\mathbf{R};0)n_u(\mathbf{R}+\mathbf{r};0)n_L(\mathbf{R}';t)n_u(\mathbf{R}'+\mathbf{r}';t)\rangle = V^{-1}\rho_u\,g(r)G_s^L(\mathbf{R}'-\mathbf{R};t)G^U(\mathbf{R}'+\mathbf{r}'-\mathbf{R}-\mathbf{r};t)g(r')\,, \tag{26}$$

and for the light scattering case

$$\langle n(\mathbf{R};0)n(\mathbf{R}+\mathbf{r};0)n(\mathbf{R}';t)n(\mathbf{R}'+\mathbf{r}';t)\rangle$$
$$=\rho^2 g(r)G(\mathbf{R}'-\mathbf{R};t)G(\mathbf{R}'+\mathbf{r}'-\mathbf{R}-\mathbf{r};t)g(r')\,. \quad (27)$$

The advantage of these approximations is that the functions $g(r)$, $G_s(r;t)$, and $G(r;t)$ are relatively well known, and can be used in the expressions for all the relevant power spectra that are experimentally accessible, of which we here derive the expression for $g_l(t)$. Substituting

$$g_l(t)=v^{-1}\rho_u \int\int\int\int d\mathbf{r}\,d\mathbf{r}'\,d\mathbf{R}\,d\mathbf{R}'$$
$$\times g(r)G_s^L(\mathbf{R}'-\mathbf{R};t)G^u(\mathbf{R}'+\mathbf{r}'-\mathbf{R}-\mathbf{r};t)g(r')$$
$$\times v_l(r)v_l(r')P_l(\mathbf{1}_r\cdot\mathbf{1}_{r'})\,, \quad (28)$$

changing to the integration variables $\Delta=\mathbf{R}'-\mathbf{R}$ and $\Delta'=\mathbf{R}+\mathbf{r}'-\mathbf{R}-\mathbf{r}$ one has to impose the condition $\Delta+\mathbf{r}'=\Delta'+\mathbf{r}$ by multiplication with

$$(2\pi)^{-3}\int \exp[i\mathbf{k}\cdot(\Delta+\mathbf{r}'-\Delta'-\mathbf{r})]\,d\mathbf{k}\,,$$

performing the integration

$$g_l(t)=(2\pi)^{-3}\rho_u \iiint d\mathbf{k}\,d\mathbf{r}'\,d\mathbf{r}\exp[i\mathbf{k}\cdot(\mathbf{r}'-\mathbf{r})]$$
$$\times g(r)\,v_l(r)g(r')\,v_l(r')\,P_l(\mathbf{1}_r\cdot\mathbf{1}_{r'})\,I_s^{L*}(k;t)\,I^u(k;t), \quad (29)$$

where $I(k;t)$ and $I_s(k;t)$ are the total intermediate scattering function and the self-part thereof. If we rewrite $\exp[i\mathbf{k}(\mathbf{r}'-\mathbf{r})]$ and $P_l(\mathbf{1}_r\cdot\mathbf{1}_{r'})$ in spherical harmonics and average over the directions of r and r' we obtain

$$g_l(t)=(2\pi)^{-3}\rho_u\int_0^\infty 4\pi k^2 V_l^2(k)\,I_s^L(k;t)\,I^u(k;t)\,dk, \quad (30)$$

where

$$V_l(k)\equiv\int_0^\infty 4\pi r^2 g(r)\,v_l(r)\,j_l(kr)\,dr,$$

in which $j_l(1r)$ is the lth spherical Bessel function.

An analogous expression can be derived starting from Eq. (27) and valid for collision induced depolarized light scattering

$$I\sim\int_0^\infty 4\pi k^2\beta^2(k)\,I^2(k;t)\,dk, \quad (31)$$

with

$$\beta(k)\equiv\int_0^\infty 4\pi r^2 g(r)\,\beta(r)\,j_2(kr)\,dr.$$

Equation (3) allows us to calculate the correlation functions $g_l(t)$ from known data of the intermediate scattering functions and the radial distribution function. The results for argon are shown in Sec. III. Two limiting cases are of interest. The first case is where the translational motion of the probe molecule is very slow compared with the translational motions of the host molecules. In that case, we may put $I_s^L(k;t)=1$ and

$$g_l(t)=(2\pi)^{-3}\rho_u\int_0^\infty 4\pi k^2 V_l^2(k)\,I^u(k;t)\,dk. \quad (32)$$

Consequently we obtain a direct relation between $\mathrm{Re}\,G_l(\omega)$ and $S^u(k,\omega)$

$$\mathrm{Re}\,G_l(\omega)=(2\pi)^{-2}\rho_u\int_0^\infty 2\pi k^2 V_l^2(k)\,S^u(k;\omega)\,dk. \quad (33)$$

If, on the other hand, the host translational motions are much slower than the probe motion, $I^u(k;t)$ may be replaced by $I^u(k;0)$. Using furthermore the Gaussian approximation

$$I_s(k;t)\approx\exp(-k^2/3)\int_0^t\int_0^{t'}\langle\mathbf{v}_L(t')\cdot\mathbf{v}_L(t'')\rangle\,dt'\,dt'',$$

we find that the time dependence of the correlation functions $g_l(t)$ is given by the velocity autocorrelation functions of the probe molecule only.

III. EXPERIMENTAL DATA

There are three sources of data on the time dependence of local anisotropies in argon; i.e., far infrared absorption measurements with a probe molecule, coherent and incoherent neutron scattering, and molecular dynamics calculations.

A. Far infrared measurements

In an earlier publication[12] the authors have reported on measurements of the HCl rotational line broadening by argon at densities ranging from 100 to 480 amagat along the 162.5 K isotherm. Due to the fact that the HCl argon system is one of the very few examples where rotational fine structure remains detectable even at liquid densities, the linewidths of the ten first pure rotational transitions could be determined. The results are given in Table I. As Eq. (17) shows, the expression for the

TABLE I. The halfwidths Γ_J in cm^{-1} of the rotational lines of HCl in argon.

$J\rightarrow J+1$	$\rho=39$ amagat	$\rho=100$ amagat	$\rho=200$ amagat	$\rho=300$ amagat	$\rho=400$ amagat	$\rho=480$ amagat
0→1		9.15±1.22				
1→2		5.89±0.18	12.31±0.66	16.4	20.0±0.6	20.1±1.8
2→3		3.57±0.19	7.26±0.49	9.3	10.0	12.2
3→4		3.41±0.11	6.42	9.2±0.5	10.8±0.2	12.5±0.6
4→5		2.66±0.1	5.3	7.51±0.24	9.74±0.8	12.0±1.8
5→6		2.09±0.22	4.07±0.27	5.67±0.37	7.13±0.17	8.01±0.24
6→7	0.61	1.65±0.16	2.67±0.22	3.91±0.24	4.65±0.37	5.58±0.3
7→8	0.52	1.21±0.19	1.92±0.13	2.46±0.36	2.86±0.57	3.23±0.16
8→9	0.32	0.87±0.06	1.38±0.29	1.54±0.32	1.72±0.24	1.88±0.17
9→10	0.33	0.57	0.67	0.62	0.91	0.85

linewidth is a linear combination of frequency components of the power spectrum of the anisotropic potential of rank l

$$\Gamma_j = \sum_i a^l_{ji}\, G_l(\omega_i). \tag{34}$$

There are reasons to assume (see below) that only $l=1$ and $l=2$ components are of any importance and hence, since the widths of ten rotational lines have been measured, the experimental data may be inverted using Eq. (34) to yield ten independent points of $G_1(\omega)$ and $G_2(\omega)$. We furthermore assume that there is no contribution from frequencies above 200 cm^{-1}, that all contributions are positive, and that alternate values of $G_1(\omega)$ and $G_2(\omega)$ can be found by a linear interpolation, this to reduce the number of unknowns. The result is shown in Fig. 2. The $\omega=0$ component of $G_1(\omega)$ cannot be obtained from the experimental linewidths, from the properties of the 3-J symbol it follows that only for l = even the zero frequency component $G_l(0)$ may contribute. The $G_1(\omega)$ components with finite ω show a well pronounced maximum around 100 cm^{-1} which, moreover, grows rapidly with increasing density. From the $G_2(\omega)$ components only $G_2(0)$ differs significantly from zero. Its values for different argon densities are plotted in Fig. 3.

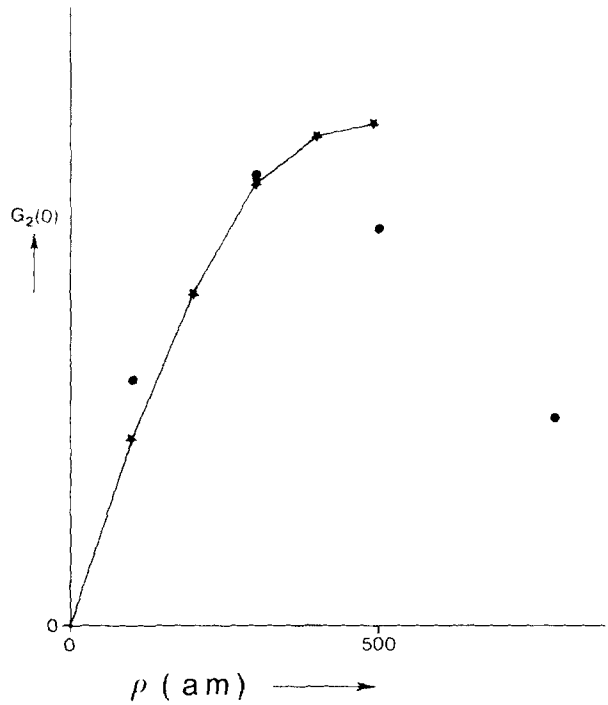

FIG. 3. Density dependence of the zero frequency component of the power spectrum of the $l=2$ anisotropic perturbation. Results from: rotational relaxation measurements (asterisks) compared with results from MD calculations (dots). Arbitrary units.

B. Neutron scattering

As follows from Eq. (30), one can calculate $G_l(\omega)$ approximately from a knowledge of the coherent and incoherent scattering functions and the radial distribution function. The only existing data in the density region of interest are from Hasman[13] on argon at a density of 304 amagat and 152.7 K. We used this data on the intermediate scattering function and on the radial distribution function[14] and a Lennard-Jones potential.[15] The resulting $G_1(\omega)$ and $G_2(\omega)$ are also shown in Fig. 2. The low limiting value of the wavevector (2.2 $Å^{-1}$) in the neutron scattering experiments makes that there is insufficient information to give any significant indication of high frequency components, a comparison with the results of the other methods is only feasible below ~40 cm^{-1}.

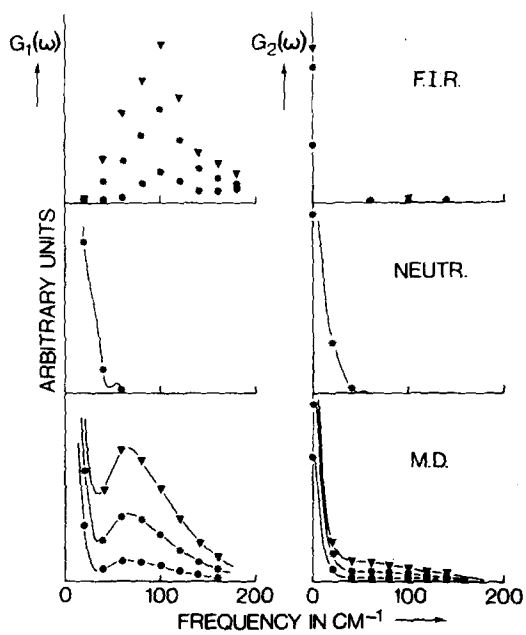

FIG. 2. Power spectra of the $l=1$ and $l=2$ anisotropic perturbation acting on a central molecule or labeled atom. Results from: far infrared rotation-relaxation measurements, neutron scattering, and MD calculations. Dots at 100 amagat density, asterisks at 300 amagat, and triangles at 480 amagat.

C. Molecular dynamics

The results of a MD calculation of the correlation functions $g_1(t)$ and $g_2(t)$ of a system which closely resembles the actual system under consideration have been published.[7] The calculations were performed for a system of 256 Lennard-Jones atoms with argon characteristics; i.e., parameter values $\epsilon = 119.5$ K and $\sigma = 3.405$ Å. The temperature corresponded to 160 K and the densities for which the calculations were performed to 100, 300, 500, and 784 amagat. The r dependence of the anisotropic potentials $v_1(r)$ and $v_2(r)$ was taken proportional to the isotropic potential. Furthermore, it was assumed that the translational motion of the atoms was not affected by the anisotropy and that all particles had the same mass. In this way every particle could successively be considered as the probe molecule, thus improving the statistics by a factor 256. The resulting correlation functions and the corresponding power spectra are shown in Figs. 2 and 4. To obtain $g_1(t)$ and $g_2(t)$ in absolute units (erg)^2 they should be multiplied by the as yet unknown well depths of the anisotropic potentials, squared. MD calculations can

easily give information with very much more detail and far more complete than the experimental methods described above. The choice of the parameter values and conditions allows a fair qualitative comparison with the results of those methods, quantitatively there are bound to be considerable differences.

IV. DISCUSSION

From Fig. 2 in which the results of three different methods are compared, it is clear that the information obtained from neutron scattering data and from rotational relaxation measurements can be largely complementary. Unfortunately, neutron scattering data are not available for more than a single density in the range of interest and we therefore restrict our discussion to the results of the rotation relaxation measurements and the MD calculations.

From Eq. (17) it follows that the rotational linewidths depend on the values of the $G_l(\omega)$ at frequencies that correspond with the level spacings in the imperturbed rotor. The properties of the 3-J symbols determine that only when l is even the zero frequency component $G_l(0)$ makes a contribution. It is, therefore, that there is no information about the zero frequency component in the G_1 as obtainable from rotational relaxation, and further, only at discrete frequencies. The MD results reproduce the characteristics of the results from relaxation measurements as well as those from the neutron scattering data. As to the density dependence, there is a very good agreement between relaxation and MD results, in particular regarding the nonlinear density dependence of the $G_2(0)$ and the strong growth of the $G_1(\omega)$ with density in the high frequency region. In this latter case, the frequency of the maximum as found from the relaxation measurements lies about 30 cm^{-1} higher than the MD calculations indicate. This might be caused by the simple fact that the MD system does not represent argon closely enough, or probably by the fact that HCl is not such an inert probe after all and does affect the translational motions in which it partakes.

A. The argon–HCl potential

In the MD calculations it was necessary for computational reasons to assume that the mass of the probe and the solvent molecule were the same, and also that the probe–host isotropic interaction potential was identical with the host–host potential. The computed correlation functions depend on the density fluctuations in the fluid that occur within the range of the $l=1$ and $l=2$ anisotropic parts of the probe–host intermolecular potential. The r dependence of these anisotropic parts of the potential was assumed to be proportional to the isotropic part. But the ratio of the contributions from the different symmetry terms ($l=1, 2, 3$, etc.) to the linewidths is of course determined by the exact r dependence of the corresponding terms in the true intermolecular potential.

The isotropic part of the HCl–Ar potential is known rather accurately.[16–18] It has a well depth of 192 K, as compared with 119 K for the Ar–Ar potential. The position of the minima of both potentials seems to be quite close. Although the difference in well depth is quite substantial, it is also true that the local structure and the short time dynamics in a dense fluid are determined predominantly by the repulsive core of the intermolecular potential. Since the repulsive parts of the Ar–Ar and the Ar–HCl potential have approximately the same range, there is reason to expect that local density fluctuations around an HCl molecule in argon will not be very different from density fluctuations around an (isoelectronic) argon atom. As for the anisotropic part of the Ar–HCl potential, it was assumed that the terms with $l \geq 3$ are of little importance for the system. Neilsen and Gordon[4] made an estimate of the $l=3$ potential term on the basis of the known multipole moments and polarizabilities of HCl and Ar. It had no noticeable effect on the computed cross sections for rotational relaxation. Hence, it seems reasonable to infer that the $l=3$ term would also be of little importance in the present calculations and might therefore be neglected. One should, however, be very cautious to reject $l \geq 3$ potential terms on the basis of an estimate that uses a multipole expansion for the intermolecular interactions. This expansion appears to converge very poorly for the short range Ar–HCl interaction and such estimates as have been made are found incompatible with the available experimental data on rotational line broadening of HCl by argon[4] and on the HCl–argon van der Waals molecule.[19]

TABLE II. Estimated depths (ϵ) and positions of the minimum (r_{min}) of the $l=1$ and $l=2$ parts of several proposed HCl–Ar anisotropic intermolecular potentials.

	$l=1$		$l=2$	
H–K, Ref. 78 Single-well	52.40	4.272	23.51	4.123
H–K, Ref. 78 Double-well	19.03	3.844	43.41	4.189
N–G, Ref. 46 Pot. 52	36.5	3.805	3.51	4.83
N–G, Ref. 46 Fully opt.	28.33	4.01	14.82	4.44
Present work	32.28	3.822	49.13	3.822
	ϵ_1 (cm^{-1})	r_{min}(Å)	ϵ_2 (cm^{-1})	r_{min}(Å)

The $l=1$ and $l=2$ part of the HCl–Ar anisotropic potential were assumed to have an r dependence given by a Lennard–Jones 6–12 potential with $\sigma = 3.405$ Å as for Ar–Ar. An obvious objection against the use of this potential for the $l=1$ part is that it does not reproduce the long-range behavior of r^{-7} correctly.[20] This discrepancy is, however, of minor importance since long-range density fluctuations contribute little to $g_1(t)$. In spite of the fact that the anisotropic interaction has been studied quite extensively[4,18,19,21] little is known with certainty about the $l=1$ and $l=2$ parts. It is not even known which of the two has the deeper minimum. A choice of the values ϵ_1 and ϵ_2 of these minima from the existing data (Table II) therefore seemed fruitless. The other way open to us was to compute the linewidth from the

TABLE III. Measured linewidths and linewidths computed with adjustable well depths ϵ_1 and ϵ_2, and the MD results by minimizing the weighted sum of squares of the differences.

	ρ = 100 amagat		ρ = 300 amagat		ρ = 480 amagat	
$J \rightarrow J+1$	exp	calc	exp	calc	exp	calc
4 → 5	2.66 ± 0.1	3.31	7.51 ± 0.24	7.51	12.0 ± 1.8	12.01
5 → 6	2.09 ± 0.22	2.28	5.67 ± 0.37	5.20	8.01 ± 0.24	7.81
6 → 7	1.65 ± 0.16	1.54	3.91 ± 0.24	3.66	5.58 ± 0.3	5.04
7 → 8	1.21 ± 0.19	1.09	2.46 ± 0.36	2.41	3.23 ± 0.16	3.36
8 → 9	0.87 ± 0.06	0.76	1.54 ± 0.32	1.55	1.88 ± 0.17	2.36

MD data using adjustable well depths ϵ_1 and ϵ_2 and minimize the weighted sum of squares of the differences between measured and computed linewidths. Using five lines with the best known widths ($J = 4-8$) and three densities (Table III) we could add a value for ϵ_1 and for ϵ_2 to Table II. These values are within the range of values given by other authors. Without assigning too much value to the numbers as such one can conclude that the real HCl–Ar potential has a rather strong $l = 2$ character, close to the Holmgren–Klemperer "double well" potential. It should be noted that the position of the minima is in general different from the value $r_{\min} = 2^{1/6}\sigma_{LJ} = 3.82$ Å to which the choice of a Lennard–Jones potential restricts us.

B. The fluctuations

The very fact that the shape of $g_1(t)$ and $g_2(t)$ depends on the density of the system is of significance. At low densities, the anisotropic potential acting on a probe is different from zero only during collisions. The correlation functions $g_l(t)$ may then be written as a sum of terms that describe the correlation of the anisotropic perturbation during a given collision and the perturbation n collisions later. Under the assumption that there is no correlation between the perturbation resulting from a given collision and the perturbation from any of the subsequent collisions, the $g_l(t)$ depend only on the time dependence of the anisotropic perturbation during an isolated binary collision. Within this approximation the shape of $g_l(t)$ does not depend on density; its size should be proportional to the collision frequency. The fact that the shape of $g_l(t)$ does depend on density implies, therefore, that there is a pronounced correlation between the anisotropic perturbations of subsequent collisions. In the impact approximation it is assumed that there is no such correlation; the evidence is that this assumption may be unjustified.

An other important point to note is that the correlation functions $g_1(t)$ and $g_2(t)$ are, at liquid densities, clearly not exponential. Exponential decay of anisotropic perturbations in liquids has been assumed by several authors,[2,3,23] specifically for the HCl–Ar system. Our results show convincingly that such an assumption is not justified.

Perhaps the most important single feature in our results is the strongly nonlinear density dependence of $G_2(0)$ as shown in Fig. 3. MD calculations, as well as relaxation measurements, show how the initial increase of $G_2(0)$ with increasing density comes to a halt around the critical density and possibly declines towards liquid densities. $G_2(0)$ is the area under the anisotropic potential correlation function $g_2(t)$ and is a measure of its effective size. Initially, at low densities, $G_2(0)$ will increase linearly with density, as the mean square size of the fluctuations will be given by

$$g_2(0) = \rho \int_0^\infty 4\pi r^2 g_0(r)\, v_2^2(r)\, dr,$$

where $g_0(r)$ is the low density pair distribution function. As long as three particle encounters are improbable, the decay time of $g_2(t)$ will be independent of density, the area under $g_2(t)$ will therefore depend linearly on ρ. At higher densities two effects will cause deviations from this behavior. First of all, the density dependence of $g_2(0)$ becomes nonlinear due to three-particle contributions

$$g_2(0) = \rho \int_0^\infty 4\pi r^2 g(r;\rho)\, v_2^2(r)\, dr + \rho^2 \int_0^\infty \int_0^\infty g^{(3)}(0, \mathbf{r}_1, \mathbf{r}_2;\ \rho) \times v_2(\mathbf{r}_1)\, v_2(\mathbf{r}_2) \cdot P_2(1_{r_1} 1_{r_2})\, d\mathbf{r}_1\, d\mathbf{r}_2,$$

where $g^{(3)}$ is the static density dependent three-particle distribution function. As the density increases the neighboring particles will tend to enclose the central molecule, thus making the angular distribution of particles more isotropic. This effect counteracts the increase of $g_2(0)$ with density. The second effect is that the decay time of $g_2(t)$ will become density dependent at higher densities. In fact τ_2 decreases by almost an order of magnitude in going from a low density gas to liquid densities which also comes about by the progressively more isotropic packing of neighbors around the central molecule. In a dilute gas an initial anisotropic perturbation decays as the perturber moves away far enough for the anisotropic potential to become effectively zero. Since the relative velocities of the particles are of the order of 3.10^4 cm s^{-1} it will take about 10^{-12} s for the particles to fly away a distance of a few Å. In the dense fluid, at the other hand, the anisotropic perturbation is large only if the probe molecule is much closer to one neighbor than to all others. The time for this perturbation to decay is of the order of the time it takes the probe to get back to the middle of the cage formed by its neighbors. As the distance involved now is typically a few tenths of an Ångstrom, the decay time may be expected to be about an order of magnitude smaller than in the dilute gas, as is indeed observed (Fig. 4).

Another important feature perceptible in the MD, as well as in the relaxation measurement results, is the rapid increase in intensity of $G_1(\omega)$ at higher frequencies as the density increases. The density dependence of $G_1(\omega)$ starts off linearly, but for densities above 300 amagat the frequency components of $G_1(\omega)$ in the region around 65 cm^{-1} (for the MD) results and more in the region around 80 cm^{-1} (for the relaxation measurements), increase much faster than linearly with increasing density. This may qualitatively be understood by noting that at high densities the probe may perform a rattling motion in the cage formed by its nearest neighbors. If the increase in high frequency components were merely

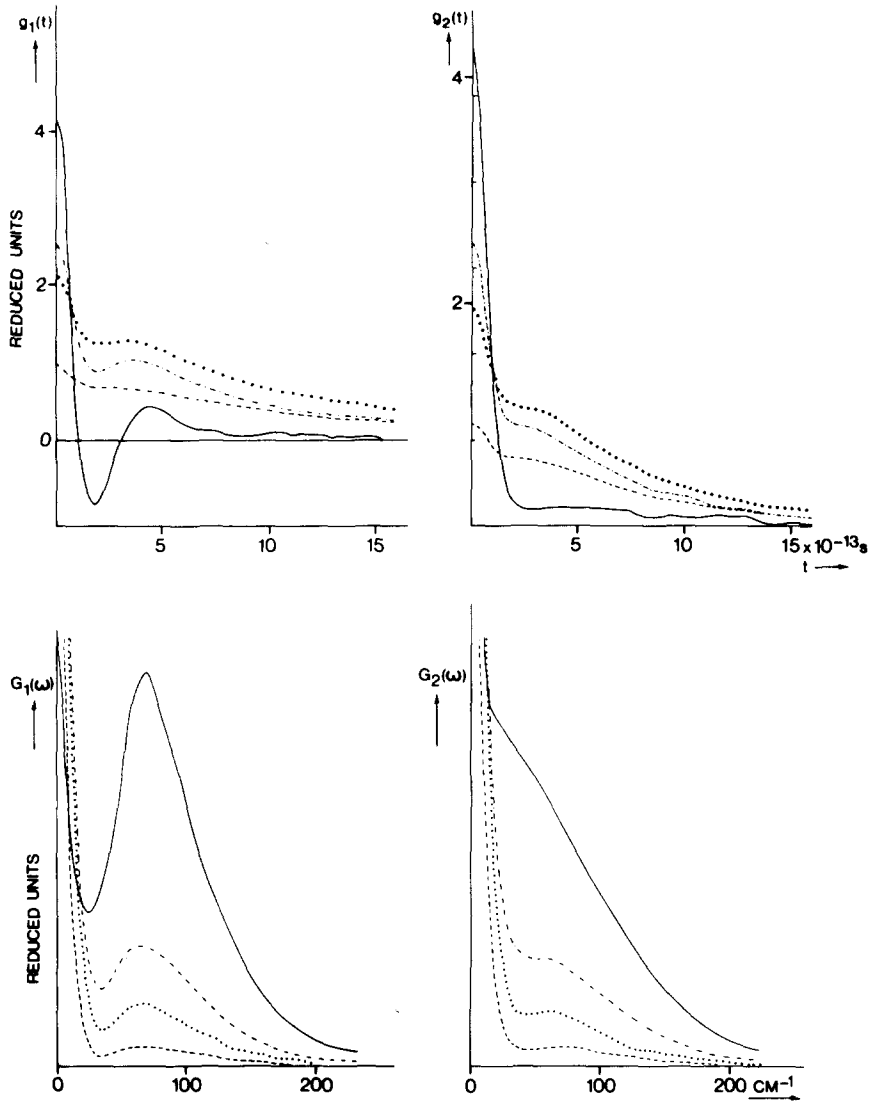

FIG. 4. The correlation functions $g_1(t)$ and $g_2(t)$ and the power spectra $G_1(\omega)$ and $G_2(\omega)$ of the $l=1$ and the $l=2$ anisotropic perturbation from MD calculations. The temperature corresponds with 162 K, the densities with 100 (-----), 300 (· · · ·), 500 (-· -·) and 784 (——) amagat units. Conversion from reduced units to erg^2 for the correlation functions through multiplication by ϵ_1^2 or ϵ_2^2; to erg^{2}s for the power spectra through multiplication by $\epsilon_1^2\tau$ or $\epsilon_2^2\tau$, where τ is $\sigma(m/48\epsilon)^{1/2}$.

due to an increase in collision frequency in the fluid, one would expect, following the Enskog approach, the ratio between linewidth Γ_j and ρ to be proportional with $g(\sigma)$, the value of the pair distribution function for contact, in the corresponding hardsphere fluid. The ratio of $g(\sigma)$ for $\rho=784$ and $\rho=100$ amagat (using $\sigma_{HS}\simeq\sigma_{LJ}$ and $g(\sigma)\simeq(2-\eta)/2(1-\eta)^3$, where $\eta=\pi\rho\sigma^3/6$)[22] is 3.78 whereas the ratio of Γ_j/ρ for lines in the region between 60 and 100 cm^{-1} is $(\Gamma_j^{784}/784)/(\Gamma_j^{100}/100)\simeq 2.5$. This lower number must be caused by a considerable destructive interference between the anisotropic interactions with different neighbors at high densities.

The rising maximum in $G_1(\omega)$ lies in the same frequency region as the maximum of the frequency distribution of liquid argon. The different behavior of $G_1(\omega)$ and $G_2(\omega)$ stems from symmetry: $P_1(\cos\Theta)$is odd in $\cos\theta$, whereas $P_2(\cos\theta)$ is even. If a particle taking part in a collective motion is close to one of its neighbors at $t=0$, it will be closer to its neighbor on the opposite side, half a period later. Consequently, choosing the z axis in the direction of the particle displacement, $g_1'(t)$ for those particles will change sign in half a period, whereas $g_2'(t)$ will not. The power spectrum of $g_1'(t)$ therefore resembles the frequency distribution of the medium closer than does the power spectrum of $g_2'(t)$. This picture is supported by the calculated behavior of $g_1(t)$ and $g_2(t)$, in particular by the evolution of $g_1(t)$ from slow monotonic decay to a rapid oscillatory behavior at the highest density.

CONCLUSIONS

Of some importance is the recognition of two possible causes for nonlinear density dependence of rotational line broadening. The first is the rapid decrease with increasing density of the decay time of local anisotropic density fluctuations in fluids. Through its anisotropic intermolecular potential, a rotating probe molecule may couple to such density fluctuations. This decrease in decay time is reflected in a much slower, rather than linear, density dependence of the $\omega=0$ part of the power spectrum of the perturbing potential on the probe. If the intermolecular potential contains even l terms, the $\omega=0$ part of the even power spectra contribute to the rotational line broadening. This contribution to the linewidths will thus cause a much slower, rather than linear, density dependence. The second cause is

coupling of the rotational motion of the probe with high frequency collective density fluctuations. This gives a contribution to the line broadening that has a faster, rather than linear, density dependence. Both effects are reflections of the fact that microscopic (high k) density fluctuations decay purely diffusively at low densities, but partly by sound propagation at high densities.

We have shown how far infrared absorption measurements of rotational linewidths of a rotor molecule surrounded by a fluid may give the values of the Fourier transforms of $g_1(t)$ and $g_2(t)$ at a finite number of discrete frequencies. Recalling the definition of $g_l(t)$ [Eq. (12)] it is evident that we will have obtained information about a number of Fourier components of the four-point density correlation function $\langle \rho(\mathbf{r};\, 0)\rho(\mathbf{r}';\, t)\rangle$. However, the information is averaged over all $\mathbf{r}$ and $\mathbf{r}'$, and there is clearly no hope of reconstructing $\langle \rho(\mathbf{r};\, 0)\rho(\mathbf{r}';\, t)\rangle$ from the experimental data. One should therefore start with a model for the four-point density correlation function and use the experimental data on rotational relaxation to test the validity of such a model. But even then one would need to know the anisotropic potential surface more accurately than it is known at present. Most experimental information on four-point density correlation functions still comes from collision induced dipolar absorption and collision induced dipolarized light scattering measurements. If, however, accurate information about the anisotropic potentials of atom–diatom systems becomes available in the future, rotational relaxation measurements on dissolved probe molecules will yield important complementary information that can be used to construct better models for four-point density correlation functions. This will greatly enhance our understanding of the details of molecular motions in dense fluids.

ACKNOWLEDGMENT

This work is part of the research program of the Foundation for Fundamental Research of Matter and was made possible by financial support from the Netherlands Organization for Pure Research.

[1]A. L. Fetter and J. D. Walecka, *Quantum Theory of Many Particle Systems* (McGraw-Hill, New York, 1971).
[2]D. Robert and L. Galatry, J. Chem. Phys. **55**, 2347 (1971).
[3]N. M. Hoang, Thèse de Doctorat (Bensançon, 1976).
[4]W. B. Neilsen and R. G. Gordon, J. Chem. Phys. **58**, 4131 (1973).
[5]A. R. Edmonds, *Angular Momentum in Quantum Mechanics* (Princeton UP, Princeton, NJ 1957). The reduced matrix elements in the present work are defined by

$$\langle jm/T(kq)/j'm'\rangle = (-1)^{j-m}(2j+1)^{1/2}\begin{pmatrix} j & k & j' \\ -m & q & m' \end{pmatrix}\langle j\|T(k)\|j'\rangle$$

[6]R. Kubo, J. Phys. Soc. Jpn. **17**, 1100 (1962).
[7]D. Frenkel and J. van der Elsken, Chem. Phys. Lett. **40**, 14 (1976).
[8]J. P. McTague, P. A. Fleury, and D. B. du Pré, Phys. Rev. **188**, 303 (1969).
[9]M. Gillan and J. Woods Halley, Phys. Rev. A **4**, 684 (1971).
[10]W. K. Holcomb and J. Woods Halley, Phys. Rev. A **7**, 694 (1973).
[11]G. H. Vineyard, Phys. Rev. **110**, 999 (1958).
[12]D. Frenkel, D. J. Gravesteyn, and J. van der Elsken, Chem. Phys. Lett. **40**, 9 (1976).
[13]A. Hasman, Physica **63**, 499 (1973).
[14]A. Hasman, Ph. D. dissertation (Delft, 1971).
[15]J. O. Hirschfelder, C. F. Curtiss, and R. B. Bird, *Molecular Theory of Gases and Liquids* (Wiley, New York, 1954).
[16]J. M. Farrar and Y. T. Lee, Chem. Phys. Lett. **26**, 428 (1974).
[17]L. Monchick, R. J. Munn, and E. A. Mason, J. Chem. Phys. **45**, 3051 (1966).
[18]S. E. Novick, K. C. Janda, S. L. Holmgren, M. Waldman, and W. Klemperer, J. Chem. Phys. **65**, 1114 (1976).
[19]A. M. Dunker and R. G. Gordon, J. Chem. Phys. **64**, 354 (1976).
[20]A. D. Buckingham, Adv. Chem. Phys. **12**, 107 (1967).
[21]U. Buck and P. McGuire, Chem. Phys. **16**, 101 (1976).
[22]N. F. Carnahan and K. E. Starling, J. Chem. Phys. **51**, 635 (1969).
[23]H. Shimizu, J. Chem. Phys. **43**, 2453 (1965).